Deciphering Expression Profiling and Functional Signatures of Individualized Obesity-Associated Genes in Ossification of Ligamentum Flavum Through RNA-Sequence Data Mining

Baoliang Zhang
Peking University Third Hospital
Lei Yuan
Peking University Third Hospital
Guanghui Chen
Peking University Third Hospital
Xi Chen
Peking University Third Hospital
Xiaoxi Yang
Peking University Third Hospital
Tianqi Fan
Peking University Third Hospital
Weishi Li
Peking University Third Hospital
Chuiguo Sun
Peking University Third Hospital
Zhongqiang Chen (puth__czq@126.com)
Peking University Third Hospital https://orcid.org/0000-0003-4423-4995

Primary research

Keywords: Bioinformatics, Gene signature, Immunity, Ossification of ligamentum flavum, Obesity

Posted Date: October 11th, 2021

DOI: https://doi.org/10.21203/rs.3.rs-955257/v1

Abstract

Background: Obese individuals predispose to ossification of ligamentum flavum (OLF), whereas the underlying connections between obesity phenotype and OLF pathomechanism are not fully understood, especially during early life. This study aimed to explore obesity-associated genes and their functional signatures in OLF.

Methods: Gene microarray expression data related to OLF were downloaded from the GSE106253 dataset in the Gene Expression Omnibus (GEO) database. The potential obesity-related differentially expressed genes (ORDEGs) in OLF were screened. Then, gene-ontology (GO) enrichment analysis and Kyoto Encyclopedia of Genes and Genomes (KEGG) pathway enrichment analysis were applied for these genes. Furthermore, protein-protein interactions (PPI) were used to identify hub ORDEGs, and Metascape was used to further verify the key signaling pathways and immune-related function signatures of hub ORDEGs. Finally, correlation analysis of hub ORDEGs and identified OLF-related infiltrating immune cells (OIICs) was constructed to understand the possible mechanical link among obesity, immune response and OLF.

Results: OLF-related differentially expressed genes and 2051 obesity-related genes from four databases were intersected to obtain 99 ORDEGs, including 54 upregulated and 55 downregulated genes. GO and KEGG analysis revealed that these genes were mainly involved in metabolism, inflammation and immune-related biological functions and pathways. A PPI network was established to determine 14 hub genes (AKT1, CCL2, CCL5, CXCL2, ICAM1, IL10, MYC, PTGS2, SAA1, SOCS1, SOCS3, STAT3, TNFRSF1B and VEGFA). The co-expression network demonstrated that this module was associated with cellular response to biotic stimulus, regulation of inflammatory response, regulation of tyrosine phosphorylation of STAT protein. Furthermore, Metascape functional annotations showed that hub genes were mainly involved in receptor signaling pathway via JAK-STAT, response to TNF and regulation of defense response, and their representative enriched pathways were TNF, adipocytokine and JAK-STAT signaling pathways. Subgroup analysis indicated that T cell activation might be potential immune function processes involved, and correlation analysis revealed that cDCs, memory B-cells and preadipocytes were highly correlated infiltrating immune cells.

Conclusions: Our study deciphered individualized obesity-associated gene signature for the first time, which may facilitate exploring the underlying cellular and molecular pathogenesis and novel therapeutic targets of obesity-related early-onset OLF.

Introduction

Ossification of ligamentum flavum (OLF) is the major pathogeny of severe thoracic myelopathy characterized by abnormally progressive heterotopic ossification of the intraspinal ligament with unelucidated pathogenesis.[1] Thoracic OLF (TOLF) prevails among East Asian population with the reported prevalence of 3.8-63.9%, which may contribute to deteriorating neurological dysfunction.[2]

Although surgical intervention could block this process, it was still accompanied by multiple complications and high surgical risks.[3,4] Therefore, it is absolutely imperative to elucidate the molecular mechanism in occurrence and development of OLF, thereby probing reliable biomarkers and novel therapeutic modalities.

To date, genetic, stress, ageing, inflammatory and metabolic factors have been found to be associated with the TOLF, whose etiological heterogeneity may indicate distinctive pathological phenotypes.[5–9] Except for susceptible middle-aged and elderly people, anecdotal observations indicated that a clinical subset of younger patients with obesity also suffered from severe or even diffuse TOLF. Additionally, concrete evidence has identified obesity as an independent causal factor for the development of TOLF in nonelderly adults.[10] Besides the systemic inflammatory state of obesity, our previous research has proven that leptin, an adipocyte-derived product encoded by Ob gene, could induce significant osteogenic differentiation in ossified ligamentum flavum cells (OLFCs), but not in normal LF cells (NLFCs), which implied that OLFCs are considerably more sensitive to leptin stimulation.[11] Therefore, we speculated the obesity-associated factors and mechanisms would participate in the progression of OLF. However, the underlying biochemical links between obesity phenotype and OLF pathogenesis have not been systematically investigated.

Multiple research strategies have been adopted to excavate the molecular mechanisms. Recently, various high-throughput sequencing technologies have gained extensive attention and provided compelling insights into OLF pathogenesis, including transcriptomics, proteomics, metabolomics and epigenetics.[9,12–14] In addition, bioinformatics analysis of gene expression profiles or other sequencing data has identified several featured genes and related biological functions of OLF.[15, 16] For instance, Wu et.al constructed key ceRNA mechanism networks and functional pathways associated with OLF using gene expression profiles.[15] Our recent work identified distinct immune-related genes and infiltrating immunocyte patterns in OLF based on transcriptome data and experiment validation, which exploited a new research direction.[16] Therefore, adopting bioinformatics algorithms for screening differentially expressed obesity-related genes and analyzing their functional signatures based on high-throughput sequencing data derived from OLF samples could help lift the veil on the underlying relationship between obesity and OLF.

In the present study, the mRNA microarray dataset GSE106253 from the Gene Expression Omnibus (GEO) was reinterpreted from other perspectives to screen the obesity-related differentially expressed genes in OLF (ORDEGs). Then, the protein-protein interaction (PPI) was constructed to further determined hub ORDEGs, and correlation analysis, co-expression analysis, gene-ontology (GO) enrichment analysis and Kyoto Encyclopedia of Genes and Genomes (KEGG) pathway enrichment analysis were applied for their functional annotations. Finally, the correlation analysis between differential infiltrating immune cells and hub ORDEGs was performed to preliminarily analyze possible immune-related functions of these genes.

Material And Methods

Collection of OLF-Related Microarray Data and Human Obesity-Related Genes Dataset

According to the inclusion criteria: 1) organism: Homo sapiens; 2) expression profiling by microarray; 3) samples: OLF ligament tissues and normal ligament tissues, an eligible high-throughput RNA-sequencing data (GSE106253) was downloaded from Gene expression Omnibus (GEO), which contains the mRNA information of ligamentum flavum tissue from 4 TOLF patients and 4 healthy individuals. Meanwhile, all obesity-related gene lists in Homo sapiens were obtained from Integratomics TIME, GWAS, T-HOD and KEGG PATHWAY databases.

Identification of OLF and Obesity-Related Differentially Expressed Genes (ORDEGs)

The raw data from GSE106253 dataset was reviewed for background correction and data normalization through the affy package of R Software. Based on the predetermined statistical threshold of |fold change| > 1 and adjusted p-values < 0.05, differentially expressed genes (DEGs) between OLF samples and healthy controls were screened out through GEO2R, an interactive online tool. Furthermore, these DEGs and ORGs were intersected to obtain the OLF-related and obesity-related DEGs (ORDEGs). Clustering heatmap and circular heatmap were performed to describe the expression of DEGs and ORDEGs, respectively.

Analyses of Gene Ontology (GO) and Kyoto Encyclopedia of Genes and Genomes (KEGG)

GO analysis was performed to annotate ORDEGs, and to illustrate their functions in biology process (BP), cell component (CC), and molecular function (MF). KEGG analysis was conducted to investigate which cellular pathways may participate in the functional alterations of ORDEGs, and to understand high-level and biological functions from large-scale molecular datasets. The clusterProfiler package was used for the GO and KEGG analysis. The cutoff values for the GO and KEGG analyses were set at $p < 0.05$.

Construction of Protein-Protein interaction (PPI) Network and Hub ORDEGs Identification

Search Tool for the Retrieval of Interacting Genes (STRING; http://string-db.org; version 11.5), an online database for predicting protein interactions, was applied to construct the PPI network of ORDEGs when interactions score > 0.7 were taken as statistically significant. Cytoscape (version 3.8.1) was used to visualize molecular interaction networks and important nodes of protein interactions within the network were further identified by ranking the scores of each node. Considering most networks were scale-free, the hub genes with degree ≥ 30 were selected. Pearson correlation analysis was performed among hub ORDEGs. Furthermore, a network of genes and their co-expression genes was analyzed via GeneMANIA4.

Functional and Correlation Analysis of Hub ORDEGs and OLF-Related Infiltrating Immune Cells (OIICs)

Metascape was used to further verify the function enrichment of hub ORDEGs with P-value < 0.05 as the cutoff. Hub genes pathway analysis was performed and visualized by ClueGO (version 2.5.8) and CluePedia (version 1.5.8). P-value < 0.01 was considered to be statistically significant. In addition, considering the obesity status is closely related to inflammation and immune response, the immune-

related function annotation of hub ORDEGs were analyzed separately using ImmuneSystemProcess in ClueGO (version 2.5.8). Finally, we conducted a correlation analysis of hub ORDEGs and OIICs to better explain the role of hub ORDEGs since 14 differential OIICs with potential effect on the development of OLF (such as with cDCs, NK CD56 bright cells, and preadipocytes) has been identified by our recent study.[16]

Statistical Analysis and Visualization

All statistical analyses and visualization were performed using R software (version 3.6.3), SPSS software and GraphPad Prism 7 software. Nonparametric test was used to examine the statistical relationship between two non-normally distributed data, and parametric test was used to examine the statistical relationship between two normal distributed data. Gene expression levels between two groups were analyzed by Student's t-test. The expression of hub ORDEGs was compared for correlation analysis using the Pearson test. All data were expressed as mean ± standard deviation. $P < 0.05$ was considered as statistically significant.

Results

Identification of ORGs in OLF

The detailed workflow diagram of this study is depicted in Figure 1. After the raw data was processed by R software for background correction and data normalization (Figure 2A), a total of 920 DEGs, consisting of 532 up-regulated genes and 388 down-regulated genes were identified between OLF samples and normal controls (Figure 2B). The clustering heatmap showed that top forty DEGs can clearly distinguish OLF tissues from normal tissues (Figure 2C). After deleting overlapping genes, a total of 2051 obesity-related gene in Homo sapiens were obtained from above four databases (Figure 2D). After intersection of these 920 DEGs and 2051 ORGs, 99 ORDEGs in OLF were ultimately identified (Figure 2E). The two-dimensional PCA depicted a significant difference in these genes to allow further analysis (Figure 2F), including 54 up-regulated genes and 55 down-regulated genes (Figure 2G). The expression profile of top 70 ORDEGs was intuitively visualized through a circular heatmap (Figure 2H).

Analysis of Go Enrichment Functions

The biological functions of up-regulated and down-regulated genes were analyzed separately (Figure 3A, 3H). GO analysis identified that the up-regulated ORDEGs were significantly enriched in BP, including hormone secretion, hormone transport and peptide hormone secretion (Figure 3B, 3C), whereas down-regulated ORDEGs were mainly enriched in regulation of lipid metabolic process, response to lipopolysaccharide and response to molecule of bacterial origin (Figure 3I, 3J). In terms of CC, up-regulated genes were mainly involved in cation-transporting ATPase complex, ATPase dependent transmembrane transport complex and mediator complex (Figure 3D, 3E) while down-regulated ORDEGs were largely enriched in phosphatidylinositol 3-kinase complex, membrane raft and membrane microdomain (Figure 3K, 3L). Moreover, MF demonstrated that up-regulated genes were mainly related to

neuropeptide hormone activity, receptor ligand activity and signaling receptor activator activity (Figure 3F, 3G), and down-regulated were mainly enriched in G protein-coupled receptor binding, phosphatase binding and nuclear receptor activity (Figure 3M, 3N). These genes could be related to multiple biological pathways orchestrating OLF pathogenesis.

Analysis of KEGG Enrichment Pathways

Analysis of lists of ORDEGs in terms of enriched biological pathways was also conducted separately for upregulated and downregulated genes. According to the enrichment analysis results of biological pathways, upregulated ORDEGs were mainly involved in collecting duct acid secretion, oxidative phosphorylation, adipocytokine signaling pathway, gastric acid secretion and cytokine-cytokine receptor interaction (Figure 4A, 4B, 4C). The top five KEGG terms among down-regulated ORDEGs were primarily associated with adipocytokine signaling pathway, mTOR signaling pathway, PPAR signaling pathway, insulin signaling pathway and JAK-STAT signaling pathway (Figure 4D, 4E, 4F). Interestingly, in upregulated and down-regulated ORDEGs, there is a common pathway, adipocytokine signaling pathway, which is implicated in multiple biological reactions (Figure 4G). Moreover, we also identified another two remarkable obesity-related crosstalk pathways, mTOR signaling pathway (Figure 4H) and JAK-STAT signaling pathway (Figure 4I). Dysregulation of module cluster genes might therefore regulate OLF development through acting on these potential pathways, which were potential signatures for OLF.

PPI Network Construction and Hub Genes Selection

To systematically analyze the relationships between the common ORDEGs, we constructed a PPI network using the STRING database after removing unconnected nodes (Figure 5A). Cytoscape visualized the PPI network of ORDEGs, which consisted of 81 nodes and 313 edges (Figure 5B). A total of 14 hub nodes (degree $\geq$ 30), including AKT1, CCL2, CCL5, CXCL2, ICAM1, IL10, MYC, PTGS2, SAA1, SOCS1, SOCS3, STAT3, TNFRSF1B, VEGFA, were considered hub genes in the OLF DEG list (Figure 5C). Table 1 shows the detailed information and molecular functions of the key genes. In addition, the result of independence testing analysis suggested that all hub genes were significantly decreased in OLF samples except for CCL5 (Figure 5D). Correlation analysis among 14 genes was further conducted to investigate their whole interrelations (Figure 5E). The results showed that SOCS3 and CCL2 had the highest positive correlation with a spearman's correlation coefficient of 0.99 (Figure 5F). STAT3 was positively correlated with SOCS3 ($r = 0.98$, Figure 5G) and VEGFA ($r = 0.98$, Figure 5H). VEGFA was also positively correlated with CXCL2 ($r = 0.98$, Figure 5I).

Analysis of the Functional Characteristics of Hub Genes

The analysis results from the GeneMANIA database showed that 14 hub genes and their co-expressed genes constitute a complex PPI network with co-expression of 65.62%, genetic interactions of 15.03%, physical interactions of 8.28%, shared protein domains of 3.99%, pathway of 3.86% and co-localization of 3.21%, whose functions were mainly associated with cellular response to biotic stimulus, regulation of inflammatory response, regulation of tyrosine phosphorylation of STAT protein (Figure 5J). Furthermore,

Metascape functional annotation results revealed that hub genes were mainly enriched in response to lipopolysaccharide, positive regulation of cell adhesion, cellular response to biotic stimulus, T cell activation, receptor signaling pathway via JAK-STAT and receptor signaling pathway via STAT (Figure 6A, 6B). Meanwhile, ClueGO revealed that the most involved pathways were JAK-STAT signaling pathway, cytokine-cytokine receptor interaction, adipocytokine signaling pathway, and chemokine signaling pathway (Figure 6C, 6D, 6E). By this token, immune-related or inflammation-related biological responses and pathways were strongly linked to these hub genes in OLF. Therefore, further subgroup analysis was conducted to separately investigate possible immune functions of these genes, and T cell activation (55.56%), cellular response to interferon-gamma (22.22%), lymphocyte migration (11.11%) and mononuclear cell differentiation (11.11%) were identified as the potential immune responses involved (Figure 6F, 6G, 6H) .

Correlation Analysis of Hub Genes and Infiltrating Immune Cells

The above results demonstrated that the hub genes were also highly enriched in immune-related or inflammation-related responses and pathways. Our previous study had identified 14 types of OLF-related infiltrating immune cells (OIICs) using ssGSEA and xCell algorithm based on the gene expression matrix from the GSE106253 (Figure 7A). To explore the underlying mechanisms associated with these potential biomarkers, we estimated the correlations between these genes and infiltration of immune cell types in OLF samples. According to $r > 0.90$ and $p < 0.001$, 27 ORDEG-OIICs correlation pairs were screened, and cDCs were significantly associated with the most ORDEGs (Figure 7B). For example, STAT3, SOCS3 and VECFA, TNFRSF1B were negatively correlated with cDCs ($r = -0.95$; $r = -0.96$; $r = -0.99$; $r = -0.95$) (Figure 7C–F); MYC, IL10 and CCL2 were negatively correlated with memory B-cells ($r = -0.97$; $r = -0.95$; $r = -0.95$) (Figure 7G-I). In addition, CCL2 and MYC were positively correlated with preadipocytes ($r = 0.96$; $r = 0.95$) (Figure 7J-K); VEGFA and CXCL2 were positively correlated with NK CD56 bright cells ($r = 0.96$; $r = 0.99$) (Figure 7L-M). These results indicated a strong correlation between the seven ORDEGs and immune cells.

Discussion

As a multifactorial disease, obesity has been considered as an important risk factor associated with the pathogenesis of OLF.[10,17] However, obesity-mediated genetic mechanism underlying the progression of OLF has not been fully understood. In this study, GSE106253 was selected as expression profiling by high-throughput sequencing dataset in our analysis. First, we screened significantly ORDEGs by intersecting OLF-related gene expression profiles and obesity-related gene lists, and their global biological functions and signal transduction pathways were analyzed. Then, fourteen hub genes were identified by constructing a protein-protein interaction network among them, and these hub genes were found to get involved in a variety of biological processes, molecular functions, signaling pathways and immune responses through correlation analysis, co-expression analysis, Metascape functional annotations, and subgroup analysis of immune function. Furthermore, we found that there was a significant correlation between the hub genes and the distinct immune cell types according to the established infiltrating immune cell patterns in OLF by our previous findings. Collectively, the current study preliminarily

investigated the expression profile of obesity-related genes in OLF and comprehensively elaborated their functional characteristics based on RNA-sequence data for the first time, which provided novel insights into understanding the pathogenesis s and treatment strategies of obesity-related OLF.

The GO and pathway enrichment analysis was of great importance for appreciating the whole biological functions and molecular mechanisms of these ORDEGs profiles in OLF. GO analysis showed that the all ORDEGs were mainly enriched in metabolic responses and obesity status. Besides, the upregulated and down-regulated ORDEGs were found to be enriched in a common KEGG pathway, adipocytokine signaling pathway, mainly including TNF-αsignaling, leptin signaling and adiponectin signaling, which is implicated in several obesity-related biological reactions. Our previous study has proven that leptin/LepR signaling could promote osteogenesis differentiation through JAK2/STAT3 pathway and indicated the intrinsic interaction between obesity and OLF 11. Moreover, our proteomics coupling with experimental verification also elucidated the definite role and mechanisms of TNF-αin development of OLF.[13,18] Besides, adiponectin signaling has been also widely involved in bone and cartilage metabolism, but contradictory results regarding its effect on bone formation and turnover were reported.[19] Numerous studies have demonstrated a pro-osteogenic potential for adiponectin in vivo in vitro through several downstream pathways.[20-23] However, Abbott et al showed that adiponectin may stimulate cellular plasticity of osteoblasts towards adipocytes.[24] Duan et al showed that AdipoRon significantly alleviates the calcification of OA chondrocytes via AMPK-mTOR signaling.[25] Generally speaking, circulating adiponectin levels are decreased in obese individuals,[26] thus it's an interesting issue whether and how adiponectin influence the development and progression of OLF. Moreover, besides JAK/STAT signaling pathway, we also identified a potential functional pathway, mTOR signaling pathway. On one hand, numerous studies have demonstrated that the mTOR activation was implicated in metabolic diseases, such as obesity and diabetes.[27,28] On the other hand, increasing mTOR signaling could promote the chondrogenesis, osteogenesis, and heterotopic ossification.[29,30] Therefore, it is speculated that mTOR signaling crosstalk may be a potential molecular mechanism linking obesity and OLF, which is worth further study in the future.

Constructing a PPI network through grouping and organizing all the genes encoding proteins is a reliable measure to screen hub genes and regulatory modules in the exploration of disease mechanism. By this means, 14 hub genes were obtained, including CCL2, SAA1, SOCS3, CXCL2, IL10, PTGS2, STAT3, SOCS1, TNFRSF1B, AKT1, ICAM1, MYC, VEGFA and CCL5. First, several cytokines or chemokines associated with inflammation and immunity were observed including CCL2, CCL5, CXCL2, IL10, PTGS2 and TNFRSF1B. For instance, Luis et al revealed that CCL2 and CCL5 participated in the immunomodulation of osteoblast differentiation during M1/M2 transition.[31] Aimalie et al found marrow adipocyte-derived CXCL2 in obese population contribute to osteolysis.[32] Generally, obesity have been shown to be associated with chronic low-grade systemic inflammation and the unspecific activation of immune system,[33] which, in turn, are believed to be associated with the onset and development of OLF. In addition, STAT3 has been verified to play an important role in the osteogenesis differentiation of ligamentum flavum cell.[11] Importantly, SOCS family proteins form part of a classical negative feedback system that regulates cytokine signal

transduction.[34] SOCS1 and SOCS3 is involved in negative regulation of cytokines that signal through the JAK/STAT3 pathway, thus they may become potential targets for progression of OLF.[35] AKT1 can regulate many processes including metabolism, cell proliferation, growth and angiogenesis, and has been demonstrated to participate in terminal stages of endochondral bone formation that is pathological nature of OLF.[36] ICAM1 has been considered as an important adhesion molecule involved in Bone Homeostasis.[37] Tanaka et al found that ICAM-1+ osteoblasts can bias bone turnover to bone resorption,[38] which prompted some novel thought about whether ICAM-1 may be potential therapeutic target for OLF. Zhang et al proposed that SAA1 was linked with progression of obesity,[39] but its role in OLF requires further verification. Yang et al indicated that angiogenesis was responsible for development of OLF.[40] VEGFA and MYC, as important participator and regulator in angiogenesis process, might be associated with advancement of OLF.[41, 42]

Based on the Metascape database, we found that the hub gene is mainly involved in biological processes such as receptor signaling pathway via JAK-STAT, response to tumor necrosis factor and regulation of defense response. ClueGO results also revealed that the most involved pathways were TNF signaling pathway, adipocytokine signaling pathway and JAK-STAT signaling pathway. These results indicated that these hub genes played an important role in inflammatory and immune response associated with obesity status in OLF. In order to further explore the role of possible immune function of these genes in OLF, we separately evaluate their involved immune response, including T cell activation, cellular response to interferon-gamma, lymphocyte migration and mononuclear cell differentiation. A previous research found differential responses of peripheral lymphocytes among patients with the continuous-type ossification of posterior longitudinal ligament (OPLL), those with the segmental-type OPLL and healthy volunteers.[43] Furthermore, transcriptomic data from calcific aortic valve disease (CAVD) samples showed increased granzyme, perforin, CD8, and interferon-gamma, supporting the presence and increased activity of T lymphocytes.[44] Moreover, interferon-gamma could specifically restrain macrophage capacity for calcium reabsorption and osteoclast activity in CAVD.[44] These findings in other types of heterotopic ossifying disease can be referenced for future research of OLF-related immunologic mechanisms. Our recent study has identified 14 types of differential OIICs,[16] so correlation analysis between hub genes and OIICs were conducted. For instance, SOCS3 and STAT3 were positively correlated with cDCs and IL10 and CCL2 were positively correlated with memory B-cells while VEGFA and CXCL2 were negatively correlated with NK CD56 bright cells. However, there is insufficient literature evidence to support these results, thus the specific mechanism of these correlations in OLF requires further experimental evidence.

The highlight of this study is to explore the expression profiles of individualized obesity-associated genes and their comprehensive function annotation in OLF for the first time. These hub genes and biological possess crosstalk may be critical for uncovering the pathogenesis of obesity-related OLF. However, there are still some limitations in this study. Due to the limited clinical samples, we are regrettably unable to verify these hub genes at this stage. In our future research, these identified target genes will be verified by RT-qPCR, western blotting or immunochemistry when clinical specimens are sufficient and ethical approval is granted. In addition, the potential mechanisms of these genes and immune cells need to be

further explored through in vitro and in vivo experiments. Importantly, we have applied scientific bioinformatics algorithm and integrated statistical methods to decipher these results within the data and show our new findings. These results, to some extent, could be enlightening for the subsequent mechanism studies.

Conclusion

Taken together, ninety-nine DEGs and fourteen hub genes associated with obesity were first identified through bioinformatics analysis for high throughput sequencing data between OLF samples and control samples. The biological functions and pathways of the identified genes provide a more detailed molecular mechanism for understanding the obesity phenotype and OLF pathogenesis. By combining a reliable deconvolution algorithm with largescale genomic data, we found significant correlation between hub genes and OIICs in OLF. Our investigations may provide new insights into the specific molecular mechanisms, diagnostic biomarkers and targeted treatment of OLF.

Abbreviations

OLF: ossification of ligamentum flavum; OLFCs: ossified ligamentum flavum cells; NLFCs: normal ligamentum flavum cells; ORDEGs: OLF-related and obesity-related differentially expressed genes; OIICs: OLF-related infiltrating immune cells; HO: heterotopic ossification; LF: ligamentum flavum; GEO: Gene Expression Omnibus; ssGSEA: single sample gene set enrichment analysis; DEGs: differentially expressed genes; GO: Gene ontology; KEGG: Kyoto Encyclopedia of Genes and Genomes; OPLL: ossification of posterior longitudinal ligament.

Declarations

Ethics approval and consent to participate

Not applicable

Consent for publication

Not applicable

Availability of data and materials

The data analyzed in this article comes from Gene Expression Omnibus (GEO) database (http://www.ncbi.nlm.nih.gov/geo). The accession number can be found in the Materials and Methods section of the article.

Competing interests

The authors declare that they have no competing interests.

Funding

This work was supported by National Natural Science Foundation of China (82072479, 81772381).

Author contributions

BLZ, LY, GHC, XC, XXY, TQF, WSL, CGS and ZQC were involved in the conception and design of the study. BLZ, LY, GHC, XC was involved in selecting the patients and in acquiring patient samples. BLZ, LY, GHC, XXY, TQF were involved in the laboratory analyses and calculating the results. BLZ, LY, CGS, WSL contributed to data interpretation. BLZ, LY, ZQC contributed to writing the manuscript. All authors revised the manuscript and approved the final version.

Acknowledgments

We thank GEO database for providing gene expression profiles of TOLF.

References

1. Zhang B, Chen G, Yang X, Fan T, Chen X, Chen Z. Dysregulation of MicroRNAs in Hypertrophy and Ossification of Ligamentum Flavum: New Advances, Challenges, and Potential Directions. Front Genet. 2021;12:641575.
2. Chen G, Fan T, Yang X, Sun C, Fan D, Chen Z. The prevalence and clinical characteristics of thoracic spinal stenosis: a systematic review. Eur Spine J. 2020;29(9):2164–72.
3. Ando K, Imagama S, Kaito T, et al. Outcomes of Surgery for Thoracic Myelopathy Owing to Thoracic Ossification of The Ligamentum Flavum in a Nationwide Multicenter Prospectively Collected Study in 223 Patients: Is Instrumented Fusion Necessary? Spine. 2020;45(3):E170–8.
4. Kim SI, Ha KY, Lee JW, Kim YH. Prevalence and related clinical factors of thoracic ossification of the ligamentum flavum-a computed tomography-based cross-sectional study. Spine J. 2018;18(4):551–7.
5. Qu X, Hou X, Chen Z, Chen G, Fan T, Yang X. Association analysis and functional study of COL6A1 single nucleotide polymorphisms in thoracic ossification of the ligamentum flavum in the Chinese Han population. Eur Spine J. 2021;10.1007/s00586-021-06932-y.
6. Cai HX, Yayama T, Uchida K, et al. Cyclic tensile strain facilitates the ossification of ligamentum flavum through β-catenin signaling pathway: in vitro analysis. Spine. 2012;37(11):E639–46.
7. Zhang B, Chen G, Chen X, Sun C, Chen Z. Cervical Ossification of Ligamentum Flavum: Elaborating an Underappreciated but Occasional Contributor to Myeloradiculopathy in Aging Population Based on Synthesis of Individual Participant Data. Clin Interv Aging. 2021;16:897–908.
8. Ren L, Hu H, Sun X, Li F, Zhou JJ, Wang YM. The roles of inflammatory cytokines in the pathogenesis of ossification of ligamentum flavum. Am J Transl Res. 2013;5(6):582–5.

9. Li J, Yu L, Guo S, Zhao Y. Identification of the molecular mechanism and diagnostic biomarkers in the thoracic ossification of the ligamentum flavum using metabolomics and transcriptomics. BMC Mol Cell Biol. 2020;21(1):37.
10. Chaput CD, Siddiqui M, Rahm MD. Obesity and calcification of the ligaments of the spine: a comprehensive CT analysis of the entire spine in a random trauma population. Spine J. 2019;19(8):1346–53.
11. Fan D, Chen Z, Chen Y, Shang Y. Mechanistic roles of leptin in osteogenic stimulation in thoracic ligament flavum cells. J Biol Chem. 2007;282(41):29958–66.
12. Han Y, Hong Y, Li L, et al. A Transcriptome-Level Study Identifies Changing Expression Profiles for Ossification of the Ligamentum Flavum of the Spine. Mol Ther Nucleic Acids. 2018;12:872–83.
13. Wang B, Chen Z, Meng X, Li M, Yang X, Zhang C. iTRAQ quantitative proteomic study in patients with thoracic ossification of the ligamentum flavum. Biochem Biophys Res Commun. 2017;487(4):834–9.
14. Fan T, Meng X, Sun C, et al. Genome-wide DNA methylation profile analysis in thoracic ossification of the ligamentum flavum. J Cell Mol Med. 2020;24(15):8753–62.
15. Wu W, Chen Y, Yang Z, et al. The Role of Gene Expression Changes in ceRNA Network Underlying Ossification of Ligamentum Flavum Development. DNA Cell Biol. 2020;39(7):1162–71.
16. Zhang B, Chen G, Chen X, et al. Integrating Bioinformatic Strategies with Real-World Data to Infer Distinctive Immunocyte Infiltration Landscape and Immunologically Relevant Transcriptome Fingerprints in Ossification of Ligamentum Flavum. J Inflamm Res. 2021;14:3665–85.
17. Endo T, Takahata M, Koike Y, Iwasaki N. Clinical characteristics of patients with thoracic myelopathy caused by ossification of the posterior longitudinal ligament. J Bone Miner Metab. 2020;38(1):63–9.
18. Zhang C, Chen Z, Meng X, Li M, Zhang L, Huang A. The involvement and possible mechanism of pro-inflammatory tumor necrosis factor alpha (TNF-α) in thoracic ossification of the ligamentum flavum. PLoS One. 2017;12(6):e0178986.
19. Lewis JW, Edwards JR, Naylor AJ, McGettrick HM. Adiponectin signalling in bone homeostasis, with age and in disease. Bone Res. 2021;9(1):1.
20. Lee HW, Kim SY, Kim AY, Lee EJ, Choi JY, Kim JB. Adiponectin stimulates osteoblast differentiation through induction of COX2 in mesenchymal progenitor cells. Stem Cells. 2009;27(9):2254–62.
21. Liu H, Liu S, Ji H, et al. An adiponectin receptor agonist promote osteogenesis via regulating bone-fat balance. Cell Prolif. 2021;54(6):e13035.
22. Chen T, Wu YW, Lu H, Guo Y, Tang ZH. Adiponectin enhances osteogenic differentiation in human adipose-derived stem cells by activating the APPL1-AMPK signaling pathway. Biochem Biophys Res Commun. 2015;461(2):237–42.
23. Wang Y, Zhang X, Shao J, Liu H, Liu X, Luo E. Adiponectin regulates BMSC osteogenic differentiation and osteogenesis through the Wnt/β-catenin pathway. Sci Rep. 2017;7(1):3652.
24. Abbott M, O'Carroll D, Wang L, Roth T, Nissenson R. Direct actions of adiponectin on mature osteoblasts may contribute to negative regulation of skeletal homeostasis. J Bone Miner Res.

2013;28:2013.
25. Duan ZX, Tu C, Liu Q, et al. Adiponectin receptor agonist AdipoRon attenuates calcification of osteoarthritis chondrocytes by promoting autophagy. J Cell Biochem. 2020;121(5-6):3333–44.
26. Landrier JF, Kasiri E, Karkeni E, et al. Reduced adiponectin expression after high-fat diet is associated with selective up-regulation of ALDH1A1 and further retinoic acid receptor signaling in adipose tissue. FASEB J. 2017;31(1):203–11.
27. Saxton RA, Sabatini DM. mTOR Signaling in Growth, Metabolism, and Disease. Cell. 2017;168(6):960–76.
28. Perl A. mTOR activation is a biomarker and a central pathway to autoimmune disorders, cancer, obesity, and aging. Ann N Y Acad Sci. 2015;1346(1):33–44.
29. Hino K, Horigome K, Nishio M, et al. Activin-A enhances mTOR signaling to promote aberrant chondrogenesis in fibrodysplasia ossificans progressiva. J Clin Invest. 2017;127(9):3339–52.
30. Wu J, Ren B, Shi F, Hua P, Lin H. BMP and mTOR signaling in heterotopic ossification: Does their crosstalk provide therapeutic opportunities? J Cell Biochem. 2019;120(8):12108–22.
31. Córdova LA, Loi F, Lin TH, et al. CCL2, CCL5, and IGF-1 participate in the immunomodulation of osteogenesis during M1/M2 transition in vitro. J Biomed Mater Res A. 2017;105(11):3069–76.
32. Hardaway AL, Herroon MK, Rajagurubandara E, Podgorski I. Marrow adipocyte-derived CXCL1 and CXCL2 contribute to osteolysis in metastatic prostate cancer. Clin Exp Metastasis. 2015;32(4):353–68.
33. de Heredia FP, Gómez-Martínez S, Marcos A. Obesity, inflammation and the immune system. Proc Nutr Soc. 2012;71(2):332–8.
34. Nicholson SE, Hilton DJ. The SOCS proteins: a new family of negative regulators of signal transduction. J Leukoc Biol. 1998;63(6):665–8.
35. Durham GA, Williams JJL, Nasim MT, Palmer TM. Targeting SOCS Proteins to Control JAK-STAT Signalling in Disease. Trends Pharmacol Sci. 2019;40(5):298–308.
36. Ulici V, Hoenselaar KD, Agoston H, et al. The role of Akt1 in terminal stages of endochondral bone formation: angiogenesis and ossification. Bone. 2009;45(6):1133–45.
37. Kong L, Yang X. Study of Intercellular Adhesion Molecule-1 (ICAM-1) in Bone Homeostasis. Curr Drug Targets. 2020;21(4):328–37.
38. Tanaka Y, Maruo A, Fujii K, et al. Intercellular adhesion molecule 1 discriminates functionally different populations of human osteoblasts: characteristic involvement of cell cycle regulators. J Bone Miner Res. 2000;15(10):1912–23.
39. Zhang X, Tang QZ, Wan AY, Zhang HJ, Wei L. SAA1 gene variants and childhood obesity in China. Lipids Health Dis. 2013;12:161.
40. Yang X, Chen Z, Meng X, et al. Angiopoietin-2 promotes osteogenic differentiation of thoracic ligamentum flavum cells via modulating the Notch signaling pathway. PLoS One. 2018;13(12):e0209300.

41. Chen D, Li Y, Zhou Z, et al. Synergistic inhibition of Wnt pathway by HIF-1α and osteoblast-specific transcription factor osterix (Osx) in osteoblasts. PLoS One. 2012;7(12):e52948.
42. Buettmann EG, McKenzie JA, Migotsky N, et al. VEGFA From Early Osteoblast Lineage Cells (Osterix+) Is Required in Mice for Fracture Healing. J Bone Miner Res. 2019;34(9):1690–706.
43. Kanai Y, Kakiuchi T. Response of peripheral lymphocytes from patients with ossification of posterior longitudinal ligament. Clin Orthop Relat Res. 2001;(389):79–88.
44. Nagy E, Lei Y, Martínez-Martínez E, et al. Interferon-γ Released by Activated CD8+ T Lymphocytes Impairs the Calcium Resorption Potential of Osteoclasts in Calcified Human Aortic Valves. Am J Pathol. 2017;187(6):1413–25.

Tables

Table 1 Detail information of 14 hub ORDEGs.

Gene symbols	Full names	Gene function	logFC	Regulation
CCL2	C-C motif chemokine 2	Chemotactic factor that attracts monocytes and basophils but not neutrophils or eosinophils. Augments monocyte anti-tumor activity. Belongs to the intercrine beta (chemokine CC) family	-3.98640165	Down
SAA1	Serum amyloid A-1 protein	Major acute phase protein; Belongs to the SAA family	-3.887612625	Down
SOCS3	Suppressor of cytokine signaling 3	SOCS family proteins form part of a classical negative feedback system that regulates cytokine signal transduction. SOCS3 is involved in negative regulation of cytokines that signal through the JAK/STAT pathway.	-3.431793	Down
CXCL2	C-X-C motif chemokine 2	Produced by activated monocytes and neutrophils and expressed at sites of inflammation. Hematoregulatory chemokine, which, in vitro, suppresses hematopoietic progenitor cell proliferation.	-2.31163825	Down
IL10	Interleukin-10	Inhibits the synthesis of a number of cytokines, including IFN-gamma, IL-2, IL-3, TNF and GM-CSF produced by activated macrophages and by helper T-cells; Belongs to the IL-10 family	-2.294065025	Down
PTGS2	Prostaglandin G/H synthase 2	Converts arachidonate to prostaglandin H2 (PGH2), a committed step in prostanoid synthesis. PTGS2 is responsible for production of inflammatory prostaglandins. Up-regulation of PTGS2 is also associated with increased cell adhesion, phenotypic changes, resistance to apoptosis and tumor angiogenesis.	-2.24627375	Down
STAT3	Signal transducer and activator of transcription 3	Signal transducer and transcription activator that mediates cellular responses to interleukins, KITLG/SCF, LEP and other growth factors. Binds to the interleukin-6 (IL-6)-responsive elements identified in the promoters of various acute-phase protein genes. Acts as a regulator of inflammatory response.	-1.792087413	Down
SOCS1	Suppressor of	SOCS family proteins form part of	-1.75724675	Down

	cytokine signaling 1	a classical negative feedback system that regulates cytokine signal transduction. SOCS1 is involved in negative regulation of cytokines that signal through the JAK/STAT3 pathway. Through binding to JAKs, inhibits their kinase activity.		
TNFRSF1B	Tumor necrosis factor receptor superfamily member 1B	Receptor with high affinity for TNFSF2/TNF-alpha and approximately 5-fold lower affinity for homotrimeric TNFSF1/lymphotoxin-alpha. This receptor mediates most of the metabolic effects of TNF-alpha. Isoform 2 blocks TNF-alpha-induced apoptosis, which suggests that it regulates TNF-alpha function by antagonizing its biological activity	-1.323437975	Down
AKT1	RAC-alpha serine/threonine-protein kinase	AKT1 is one of 3 closely related serine/threonine- protein kinases (AKT1, AKT2 and AKT3) called the AKT kinase, and which regulate many processes including metabolism, proliferation, cell survival, growth and angiogenesis. This is mediated through serine and/or threonine phosphorylation of a range of downstream substrates.	-1.270291	Down
ICAM1	Intercellular adhesion molecule 1	CAM proteins are ligands for the leukocyte adhesion protein LFA-1 (integrin alpha-L/beta-2).	-1.214991212	Down
MYC	Myc proto-oncogene protein	Transcription factor that binds DNA in a non-specific manner. Activates the transcription of growth-related genes. Binds to the VEGFA promoter, promoting VEGFA production and subsequent sprouting angiogenesis.	-1.189989425	Down
VEGFA	Vascular endothelial growth factor A	Growth factor active in angiogenesis, vasculogenesis and endothelial cell growth. Induces endothelial cell proliferation, promotes cell migration, inhibits apoptosis and induces permeabilization of blood vessels.	-1.181641133	Down
CCL5	C-C motif chemokine 5	Chemoattractant for blood monocytes, memory T-helper cells and eosinophils. Causes the release of histamine from basophils and activates eosinophils. May activate several	1.378546375	Up

chemokine receptors including CCR1, CCR3, CCR4 and CCR5.

Abbreviations: ORDEGs, obesity-related differentially expressed genes.

Figures

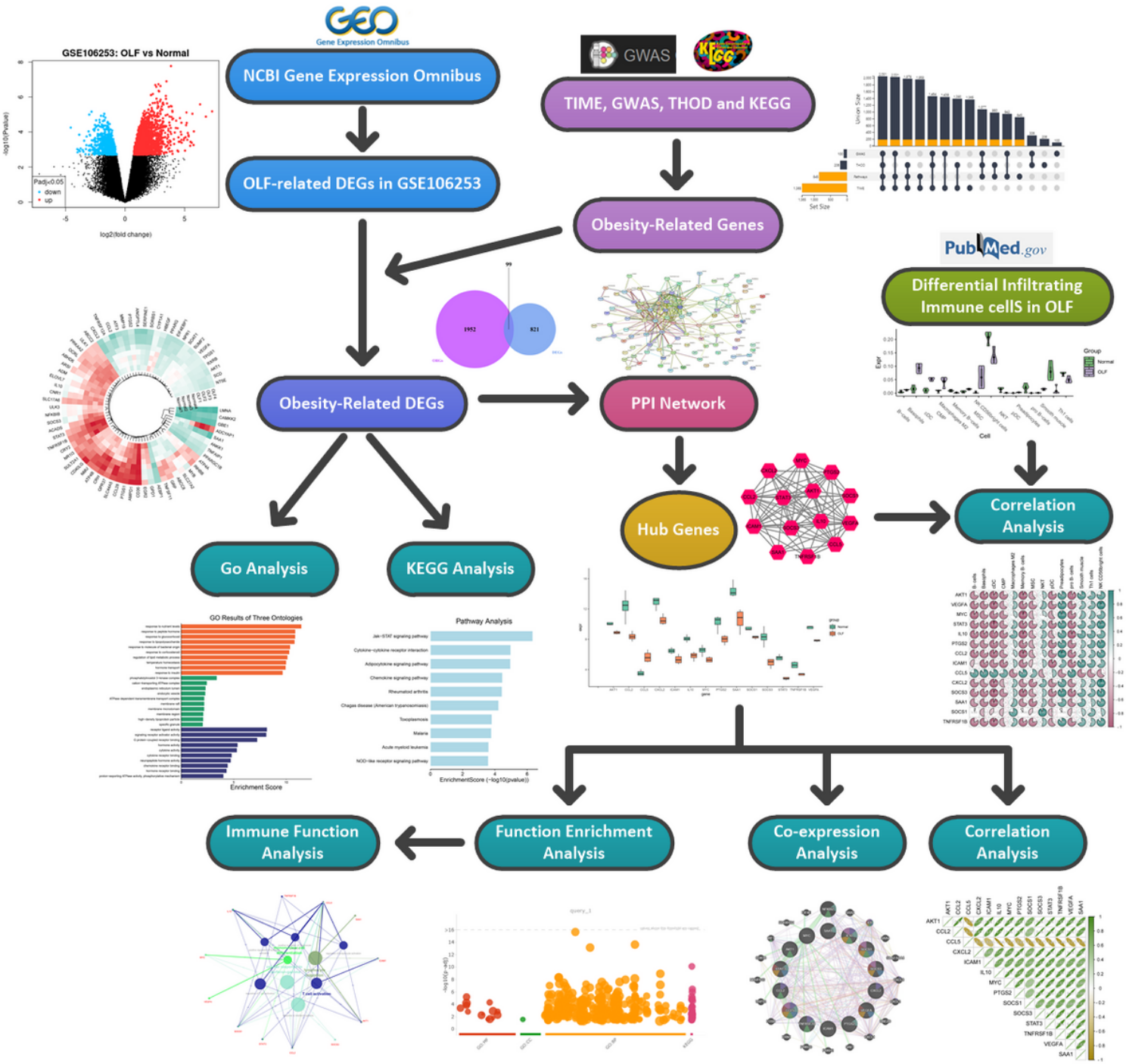

Figure 1

Flow chart of the whole analysis process.

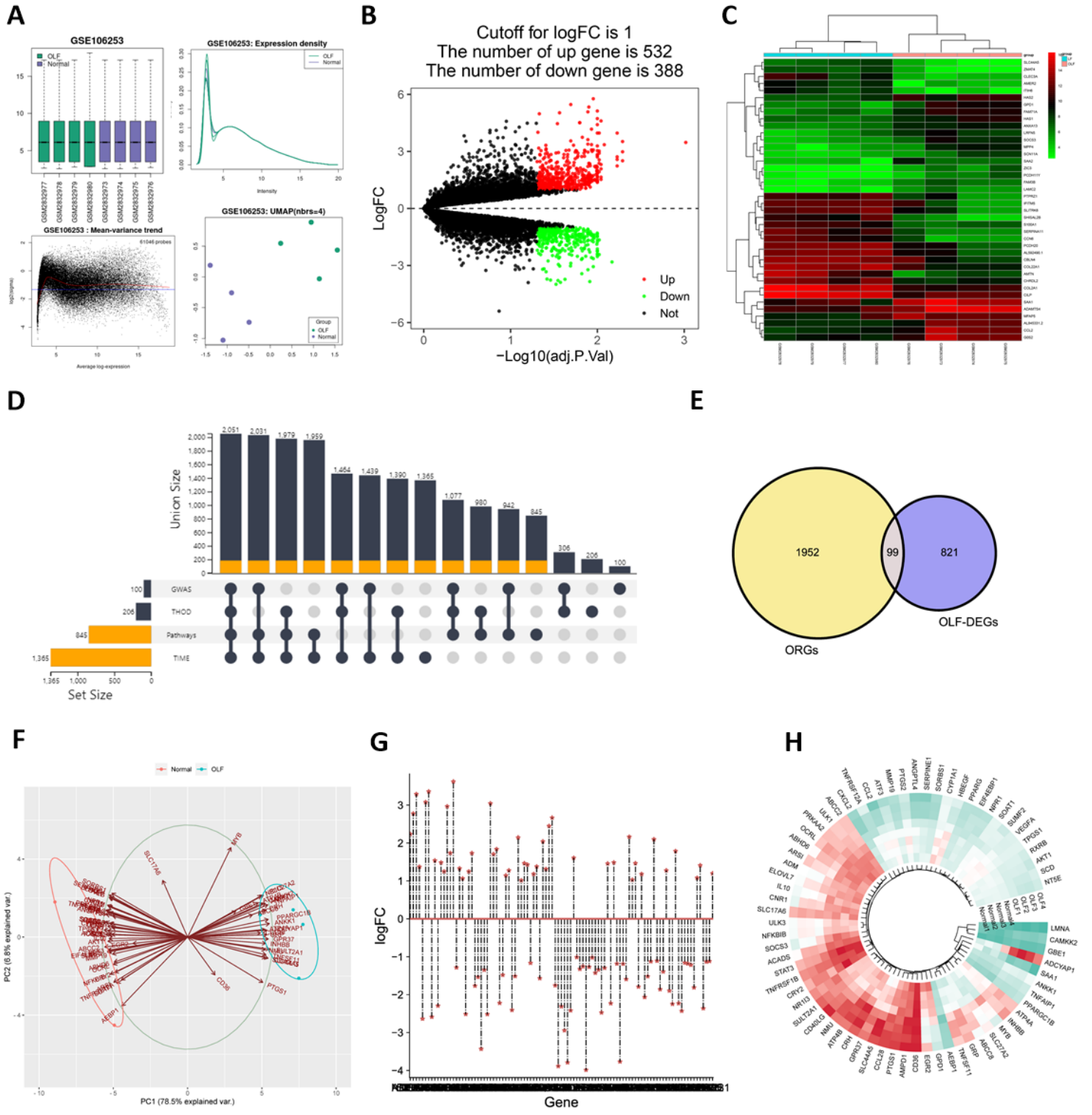

Figure 2

Identification and analysis of obesity-related DEGs in OLF. (A) The raw data was processed by R software for background correction and data normalization. (B) Volcano map of 920 DEGS, including 532 up-regulated genes and 388 down-regulated genes. Magenta dots represent genes with |logFC| > 1 and adj.P value < 0.05. The red nodes represent upregulated DEGs and green nodes represent downregulated DEGs;

the black nodes represent genes with p-value > 0.05. (C) The two-way hierarchical clustering heatmap of top 40 genes. Each column in the heatmap represents a sample, and each row represents a gene. (D) A total of 2051 obesity-related gene lists in Homo sapiens were obtained from Integratomics TIME, GWAS, T-HOD and KEGG PATHWAY databases. (E) Venn diagram indicates the overlap of DEGs in OLF and obesity-related genes to obtain 99 ORDEGs. (F) The two-dimensional PCA depicted a significant difference in 99 ORDEGs. (G) Stem-and-Leaf Plot showed the expression change of 99 ORDEGs, including 54 up-regulated genes and 55 down-regulated genes. Horizontal axes represent genes, and vertical axes represents fold change. (H) Circular heatmap showed the expression profile of top 70 ORDEGs.

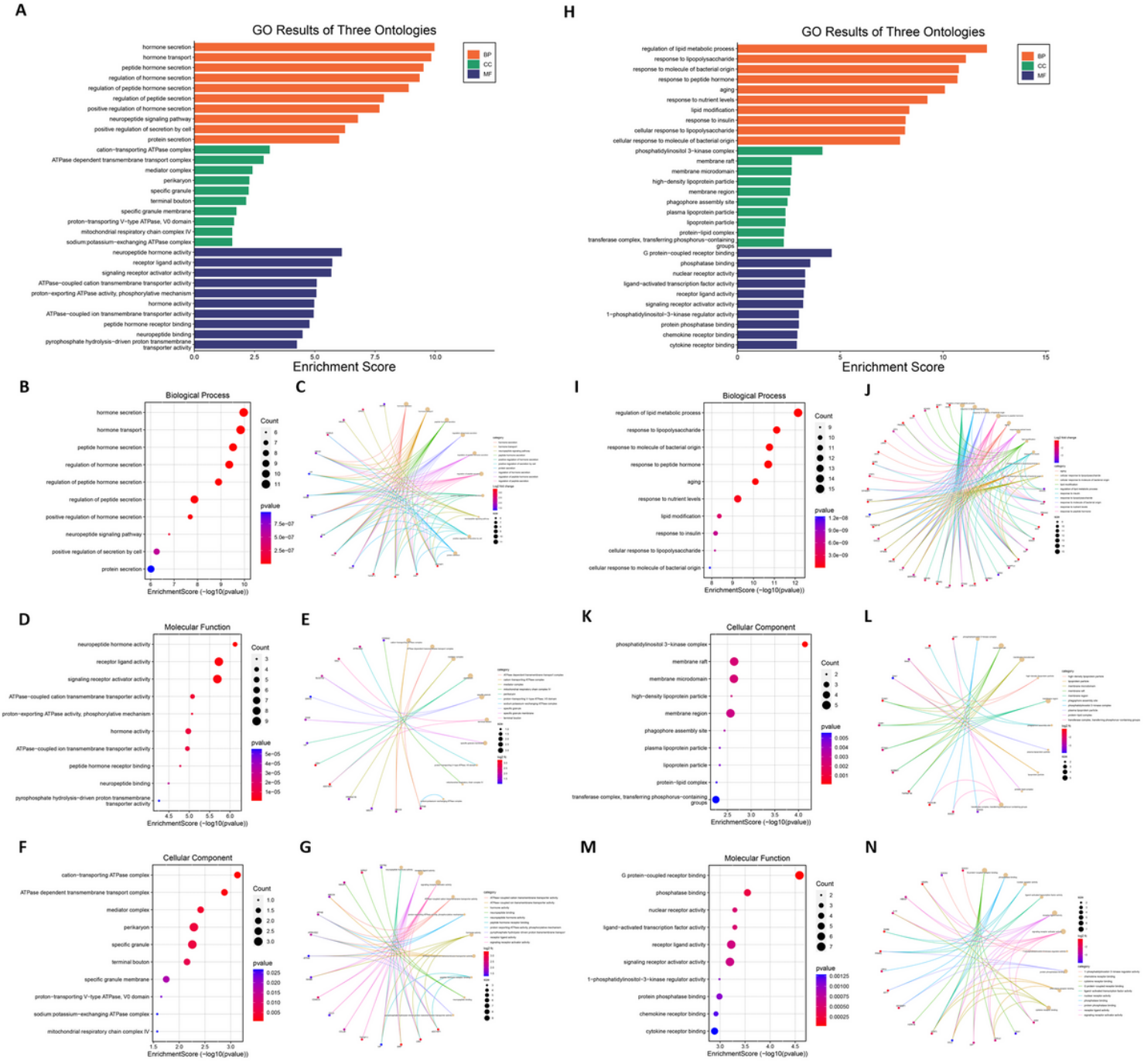

Figure 3

GO analyses of the upregulated and downregulated ORDEGs between OLF and control samples. (A) GO histogram plot showed the enriched functions of upregulated genes in biological processes (BP), cellular components (CC), and molecular functions (MF). (B) GO bubble plot showed the enriched functions of upregulated genes in BP. (C) GO cnetplot showed the enriched functions of upregulated genes in BP. (D) GO bubble plot showed the enriched functions of upregulated genes in MF. (E) GO cnetplot showed the enriched functions of upregulated genes in MF. (F) GO bubble plot showed the enriched functions of upregulated genes in CC. (G) GO cnetplot showed the enriched functions of upregulated genes in CC. (H) GO histogram plot showed the enriched functions of downregulated genes in biological processes (BP), cellular components (CC), and molecular functions (MF). (I) GO bubble plot showed the enriched functions of downregulated genes in BP. (J) GO cnetplot showed the enriched functions of downregulated genes in BP. (K) GO bubble plot showed the enriched functions of downregulated genes in MF. (L) GO cnetplot showed the enriched functions of downregulated genes in MF. (M) GO bubble plot showed the enriched functions of downregulated genes in CC. (N) GO cnetplot showed the enriched functions of downregulated genes in CC.

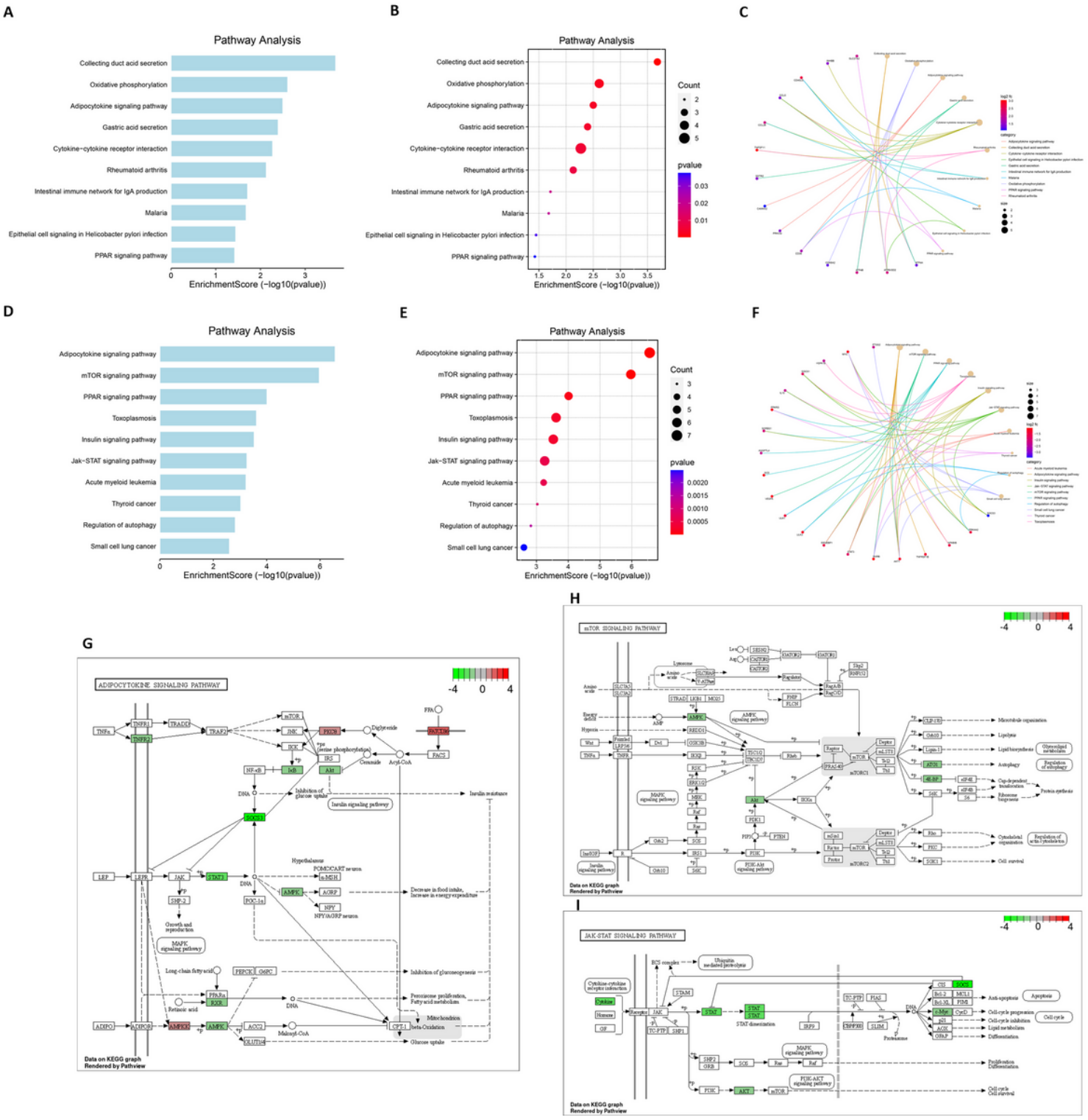

Figure 4

KEGG analyses of the upregulated and downregulated ORDEGs between OLF and control samples. (A) KEGG histogram plot showed the enriched pathways of upregulated genes. (B) KEGG bubble plot showed the enriched pathways of upregulated genes. (C) GO cnetplot showed the enriched pathways of upregulated genes. (D) KEGG histogram plot showed the enriched pathways of downregulated genes. (E) KEGG bubble plot showed the enriched pathways of downregulated genes. (F) KEGG cnetplot showed the

enriched pathways of downregulated genes. (G) The map of the adipocytokine signaling pathway. (H) The map of the mTOR signaling pathway. (I) The map of the JAK-STAT signaling pathway.

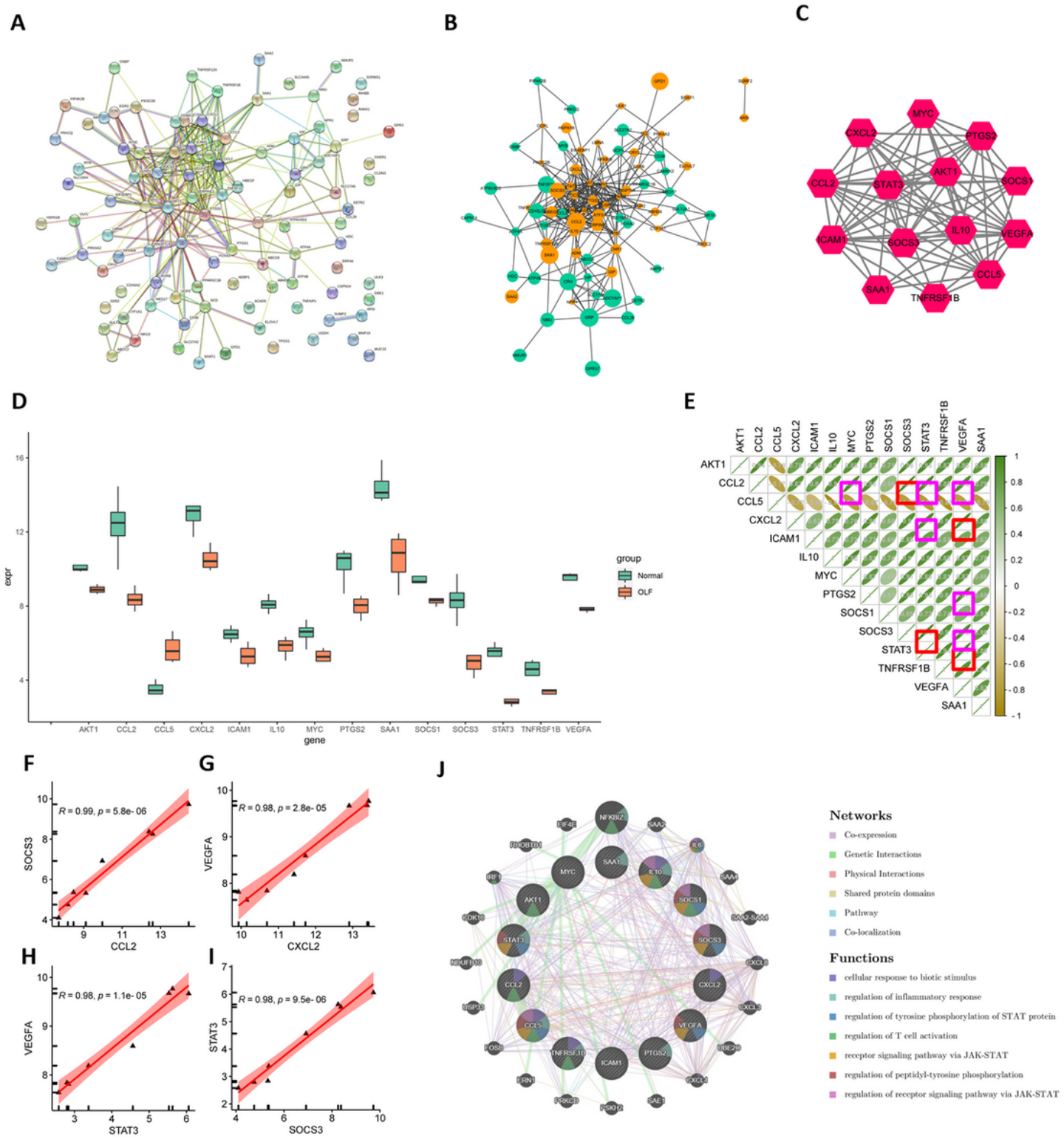

Figure 5

Protein-Protein interaction network construction and modular analysis. (A) Construction of the PPI network based on all 99 ORDEGs in STRING 11.5. (B) The PPI network of these ORDEGs was displayed in the Cytoscape software. Up-regulated genes are marked in light green; down-regulated genes are marked

in light orange. (C) The most important module composed of hub genes. (D) Box plot showed 14 hub genes expression level between OLF and control samples. (E) Correlation heatmap of 14 hub genes. The number represents the correlation coefficient, green represents the positive correlation, and yellow represents the negative correlation. (F) SOCS3-CCL2 correlation. (G) VEGFA-CXCL2 correlation. (H) VEGFA-STAT3 correlation. (I) STAT3-SOCS3 correlation. (J) Hub genes and their co-expression genes were analyzed using GeneMANIA.

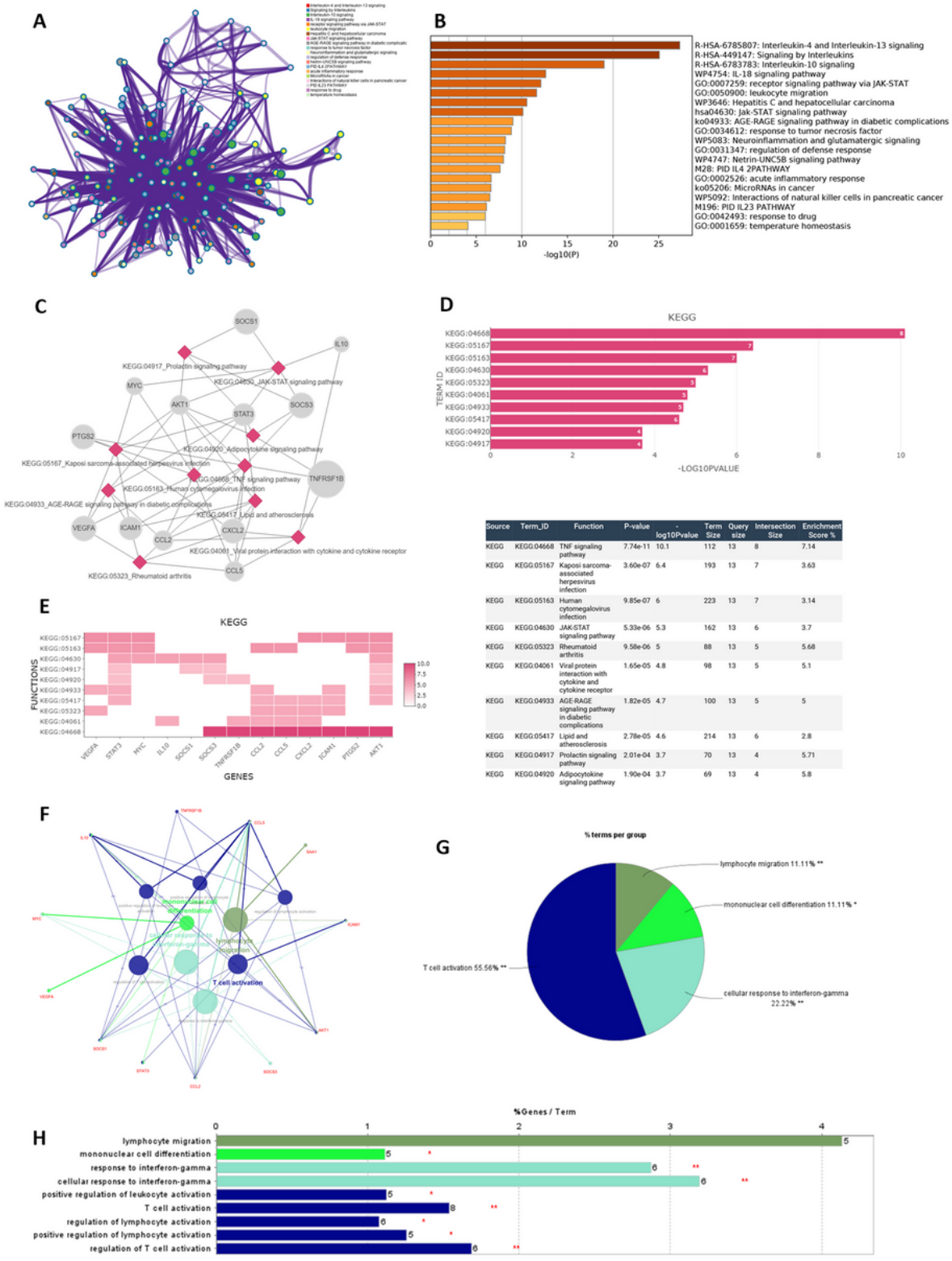

Source	Term_ID	Function	P-value	-log10Pvalue	Term Size	Query size	Intersection Size	Enrichment Score %
KEGG	KEGG:04668	TNF signaling pathway	7.74e-11	10.1	112	13	8	7.14
KEGG	KEGG:05167	Kaposi sarcoma-associated herpesvirus infection	3.60e-07	6.4	193	13	7	3.63
KEGG	KEGG:05163	Human cytomegalovirus infection	9.85e-07	6	223	13	7	3.14
KEGG	KEGG:04630	JAK-STAT signaling pathway	5.33e-06	5.3	162	13	6	3.7
KEGG	KEGG:05323	Rheumatoid arthritis	9.58e-06	5	88	13	5	5.68
KEGG	KEGG:04061	Viral protein interaction with cytokine and cytokine receptor	1.65e-05	4.8	98	13	5	5.1
KEGG	KEGG:04933	AGE-RAGE signaling pathway in diabetic complications	1.82e-05	4.7	100	13	5	5
KEGG	KEGG:05417	Lipid and atherosclerosis	2.78e-05	4.6	214	13	6	2.8
KEGG	KEGG:04917	Prolactin signaling pathway	2.01e-04	3.7	70	13	4	5.71
KEGG	KEGG:04920	Adipocytokine signaling pathway	1.90e-04	3.7	69	13	4	5.8

Figure 6

The function analysis of hub genes. (A-B) The functions of hub genes were mainly enriched in receptor signaling pathway via JAK-STAT, response to tumor necrosis factor and regulation of defense response. (C-E) The most significant pathway and related genes. The results show that these hub genes are mainly involved in JAK-STAT signaling pathway, cytokine-cytokine receptor interaction, adipocytokine signaling pathway, and chemokine signaling pathway. (F-H) The most significant immune response and related genes. The results show that these hub genes are mainly involved in T cell activation, cellular response to interferon-gamma, lymphocyte migration and mononuclear cell differentiation.

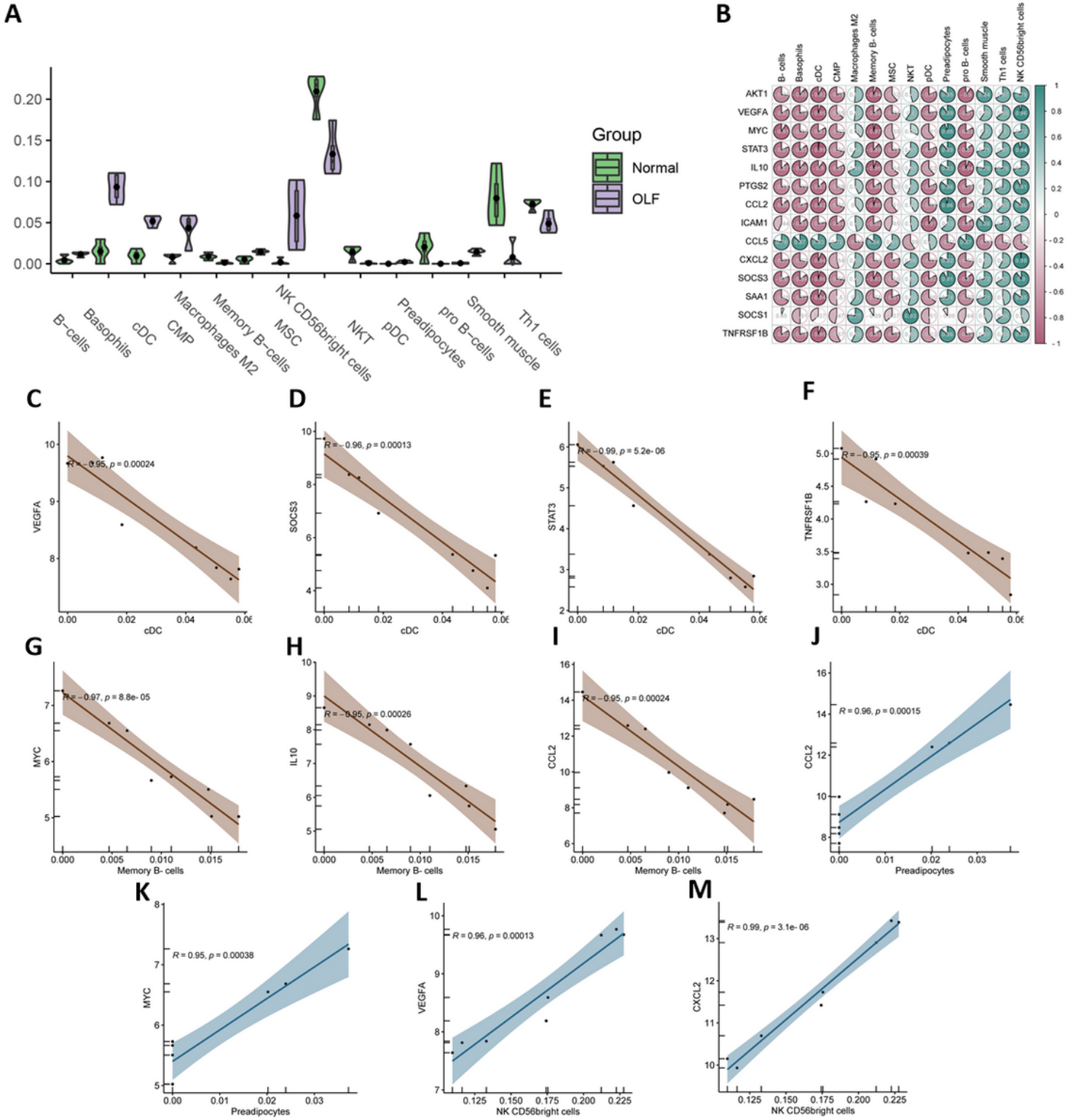

Figure 7

Correlation analysis between OIICs and ORDEGs. (A) Violin plot showed the infiltrating level of identified 14 types of immune cells between OLF and control samples. (B) Correlation heat map between hub genes and immune cells. The number represents the correlation coefficient, red represents the positive correlation, and green represents the negative correlation. (C) VEGFA-cDC correlation. (D) SOCS3-cDC correlation. (E) STAT3-cDC correlation. (F) TNFRSF1B-cDC correlation. (G) MYC-memory B-cells correlation. (H) IL10-memory B-cells correlation. (I) CCL2-memory B-cells correlation. (J) CCL2-preadipocytes correlation. (K) MYC-preadipocytes correlation. (L) VEGFA-NK CD56bright cells correlation. (M) CXCL2-NK CD56bright cells correlation.